HHS Public Access

Author manuscript

Circ Res. Author manuscript; available in PMC 2022 October 01.

Published in final edited form as:

Circ Res. 2021 October ; 129(8): e166–e182. doi:10.1161/CIRCRESAHA.121.319104.

atg7-Based Autophagy Activation Reverses Doxorubicin-Induced Cardiotoxicity

Yong Wang[1,2,3,*], **Xiaoguang Lu**[1,2,4,*], **Xiaoping Wang**[3,*], **Qi Qiu**[1,2,5], **Ping Zhu**[1,2], **Lin Ma**[3], **Xiao Ma**[1,2], **Joerg Herrmann**[2], **Xueying Lin**[1,2], **Wei Wang**[3], **Xiaolei Xu**[1,2]

[1]Biochemistry and Molecular Biology, Mayo Clinic, Rochester, Minnesota, USA

[2]Cardiovascular Medicine, Mayo Clinic, Rochester, Minnesota, USA

[3]School of Traditional Chinese Medicine, Beijing University of Chinese Medicine, Beijing, China

[4]Dongzhimen Hospital, Beijing University of Chinese Medicine, Beijing, China

[5]Institute of Clinical Pharmacology, Beijing Anzhen Hospital, Capital Medical University, Beijing, China.

Abstract

Rationale: Anthracycline-induced cardiotoxicity (AIC) is a major side effect that limits the use of anthracyclines as effective chemotherapeutics. No mechanism-based therapy is available when cardiac function deteriorates.

Objective: We aim to elucidate the dynamic autophagic defects in AIC, and to identify a mechanism-based therapy via both genetic and pharmacological studies.

Method and Results: Through phenotyping an adult AIC (aAIC) zebrafish model, we detected a biphasic response in autophagy: activation in the early stage and suppression in the later phase that is characterized by a decline in cardiac function. We conducted conditional genetic studies with *atg7*, which encodes a rate-limiting autophagy core protein, and found that *atg7* overexpression (OE) leads to therapeutic effects in the late phase but deleterious effects in the early phase of aAIC. We then assessed the therapeutic effects of 37 FDA-approved autophagy activators (FAAs) using an embryonic AIC (eAIC) zebrafish model and identified spironolactone, pravastatin, and minoxidil as top-ranking drugs. We demonstrated the therapeutic efficacy of these FAAs in the aAIC model and confirmed that these drugs exert therapeutic effects in the late phase but not in the early AIC phase. Finally, we demonstrated that the time-dependent therapeutic

Address correspondence to: Dr. Xiaolei Xu, Department of Biochemistry and Molecular Biology, Department of Cardiovascular Medicine, Mayo Clinic, 200 First Street SW, Rochester, Minnesota, 55905, USA, Tel: +1(507)284-0685, xu.xiaolei@mayo.edu., Dr. Wei Wang, School of Traditional Chinese Medicine, Beijing University of Chinese Medicine, No. 11, North 3rd Ring East Road, Chaoyang District, Beijing, 100029, China., Tel: +86(010)6428-6508, wangwei26960@126.com.

*These authors contributed equally to this work.

DISCLOSURES

None.

effects are conserved in a mouse AIC model and that spironolactone and rapamycin activated autophagy in an Atg7-dependent fashion.

Conclusions: Our findings suggest that atg7-based autophagy activation is an effective therapeutic avenue to reversing the decline in cardiac function in AIC, highlighting the time dependent nature of autophagy-based therapy.

Graphical Abstract

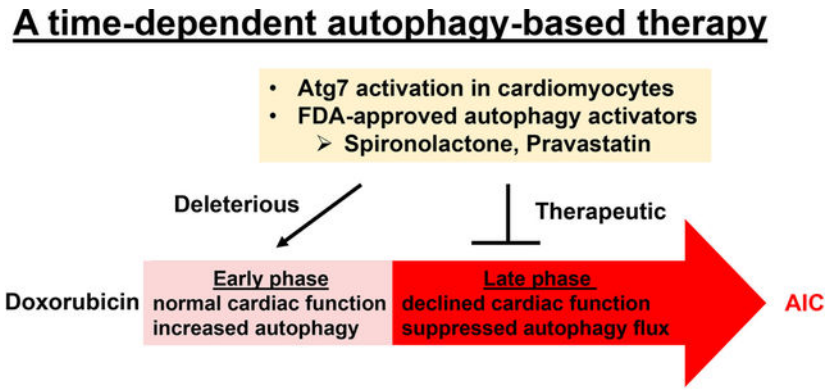

Keywords

Animal Models of Human Disease; Cardiotoxicity; Cardio-Oncology; Genetics; Translational Studies

INTRODUCTION

Anthracyclines, including doxorubicin (DOX), are effective antitumor drugs. However, the utility of anthracyclines is compromised by their dose-dependent cardiotoxicity.[1] Anthracycline-induced cardiotoxicity (AIC) has been categorized into acute and chronic forms.[2] Acute AIC typically manifests as acute (toxic) myocarditis in <1% of patients and is considered to be self-limiting. On the other hand, chronic AIC occurs months or years after therapy and leads to a decline in cardiac function, which can progress to heart failure (HF). The administration of generic HF therapies such as β-blockers and ACE inhibitors is currently the only available remedy, leading to full recovery of cardiac function in only 10% of patients.[3, 4] Therefore, there remains a great need to gain more insight into the underlying mechanisms of AIC and to develop new therapeutic strategies.[5]

Topoisomerase (Top) 2b has been recently identified as a key molecular target of DOX.[6] Through direct binding to Top 2b, anthracyclines induce DNA double-stranded breaks that lead to cardiomyocyte death.[5] Dexrazoxane, an iron chelator that has been developed as a cardioprotective agent, prevents anthracyclines-induced DNA damage via depleting both Topoisomerase 2 isoforms. [7] Despite the only mechanism-based Food and Drug Administration (FDA)-approved drug for treating AIC,[8] dexrazoxane is approved only for treating adults with metastatic breast cancer who need additional doxorubicin to maintain tumor control.[2] No effective drug is available to reverse chronic AIC when cardiac function has already deteriorated.

Autophagy is a vital machinery for protein quality control that plays an important role in clearing misfolded proteins and damaged organelles.[9] Dysregulated autophagy has been reported in many types of cardiomyopathies, including AIC.[9, 10] Depleted cellular TFEB, a master transcription factor that regulates lysosomal genes, has been found to be critical for DOX-induced myocyte injury.[11] Using an improved mouse model of AIC with less side effects, Li et al recently reported blunted autophagic flux, possibly a consequence of impaired lysosome acidification and lysosomal function.[12] Despite consensus that autophagy dysregulation is an important pathological event in AIC, methods to repair autophagy for therapeutic effects remain to be discovered. A pharmacological study in rats reported that six weeks of calorie restriction combined with resveratrol induced autophagy and protected the rat hearts against DOX-induced toxicity.[13] However, Li et al conducted genetic studies of Beclin 1, a PI3K that governs autophagy initiation, and noted therapeutic effects of *Beclin1+/−* in a mouse AIC model,[12] suggesting a therapeutic benefit of depressing autophagy. These results underscore the complexity of autophagy dysregulation, AIC pathogenesis, and the combination of both, beckoning further mechanistic insights for developing an effective autophagy-based therapy.

Zebrafish is a novel vertebrate model that has recently been used for studying AIC. An embryonic AIC (eAIC) zebrafish model has been used to screen compound libraries, leading to the discovery of visnagin, which mitigates the activation of cytochrome P450 family 1 (CYP1) that is induced by DOX.[14, 15] To recapitulate the progressive pathological process in human AIC, we developed an adult AIC (aAIC) model in zebrafish.[16] Injection of a single bolus of DOX into adult zebrafish resulted in cardiac dysfunction 4 weeks post injection (wpi), which becomes increasingly severe by 8 wpi. Intriguingly, we noted dynamic mTOR and autophagy dysregulation in this aAIC model, i.e., increased LC3-II expression during the first wpi but reduced LC3-II in the later phase of AIC 12 wpi.[17] Consistent with time-dependent signaling, *mtor* inhibition via rapamycin administration exerted deleterious effects in the early phase but therapeutic effects in the late phase.

Because autophagy is a critical downstream signaling branch of mTOR, here, we directly tested the potential time-dependent functions of autophagy in AIC via genetic studies of *atg7* and pharmacological studies of FDA-approved autophagy activators (FAAs). *atg7* encodes a rate-limiting protein involved in the initiation of autophagy, functioning as an ATP-binding and catalytic site for E1 proteins that activate two ubiquitin-like proteins, Atg8 and Atg12.[18] Similar to mTOR inhibition, which leads to therapeutic effects in a spectrum of cardiomyopathies, Atg7 overexpression has been shown to activate autophagy and to ameliorate pressure overload (PO)-induced cardiac dysfunction and desmin-related cardiomyopathy.[19–21] We obtained *atg7*-knockout mutant zebrafish, generated a transgenic fish line that overexpresses *atg7* in a temporally controlled manner, and then assessed the modifying effects of FAAs on a zebrafish aAIC model.[16] We confirmed our findings in a mouse AIC model, which established *atg7*-based autophagy activation as an effective therapeutic avenue to reversing the decline in cardiac function in AIC.

METHODS

Data Availability.

The data that support the findings of this study are available from the corresponding author on reasonable request. Please see the Major Resources Table in the Supplemental Materials. An expanded version of the Methods section is presented in the online Data Supplementary.

RESULTS

Autophagy is activated in the early phase but suppressed in the late phase in the adult AIC (aAIC) zebrafish model.

To define the dynamics of autophagic defects in the heart of a zebrafish aAIC model (Fig 1A and B), we assessed basal autophagy by quantifying the LC3-II protein at different phases of pathogenesis, and autophagic flux by applying bafilomycin A1 (BafA1) 4 h before sample collection. Myofibril defects were noted in this model at both histological and ultrastructural levels at 4 wpi, which became more obvious at 8 wpi (Online Fig IA and B). Because the decreased EF was significant at 4 wpi (Fig 1B), we decided to use this time point to distinguish the early and late phase of aAIC. At one day post-injection (dpi), we noted significantly increased LC3-II levels and an increased response to BafA1, suggesting both increased basal autophagy and autophagic flux (Fig 1C, D and E). In contrast, at 8 weeks post injection (wpi), the basal level of LC3-II was reduced, and the LC3-II ratio between groups treated with and without BafA1 decreased, suggesting attenuated basal autophagy and blunted autophagic flux (Fig 1C, F and G). To validate the observation obtained by Western blotting, we utilized *Tg(GFP-Lc3)* transgenic fish, which enabled us to perform an in vivo analysis of autophagic dynamics in cardiomyocytes. Consistent with the Western blot analysis results, we observed more GFP-positive puncta, indicative of autophagosomes, in the heart section 1 dpi, as well as an increased number of puncta after BafA1 treatment. In contrast, fewer GFP-positive puncta and an attenuated response to BafA1 were noted in the hearts 8 wpi (Online Fig IC and D). These data indicate a biphasic alteration in autophagic activity in the early and late phases of aAIC.

While atg7+/− exerts salutary effects in aAIC, atg7 overexpression (OE) exerts deleterious effects in the early phase of aAIC.

To interrogate the functions of autophagy in aAIC, we obtained an *atg7*^{sa10973} mutant (hereafter referred to as *atg7*).[22] While homozygous *atg7−/−* zebrafish die during the larva-juvenile transition period with severe cardiac pathology and gastrointestinal tract developmental defects,[23, 24] heterozygous *atg7+/−* zebrafish appear normal until at least 2 years of age. We noted reduced LC3-II expression in the *atg7+/−* hearts and a reduced response to BafA1 treatment (Fig 1H, I and J), suggesting attenuated basal autophagy and autophagic flux. To assess the impact of *atg7* haploinsufficiency on aAIC, we injected 20 mg/kg DOX into four-month-old *atg7+/−* zebrafish. While no significant change in EF was noted 1 wpi (Online Fig IID), a salutary effect was detected in the *atg7*+/− zebrafish 8 wpi, as indicated by mild but significant improvement in EF (Fig 1K). Consistent with the cardioprotective effect of *atg7* haploinsufficiency on aAIC, DOX-induced induction of *nppa*

and *nppb*, two molecular markers of cardiac remodeling, was attenuated in *atg7+/−* zebrafish (Fig 1L).

To assess atg7 gain of function, we generated *Tg(βactin2: loxP-mCherry-stop-loxP-atg7-cerulean)* zebrafish, referred to as *Tg(βact2:atg7)* zebrafish. A founder of the *Tg(βact2: atg7)* line was bred to a *Tg(cmlc2:CreER)* line zebrafish to generate *Tg(βact2:atg7);Tg(cmlc2:CreER)* double-transgenic fish, also termed *atg7;cre*. To induce gene overexpression, we incubated the double-transgenic fish with 1 μM 4-hydroxytamoxifen (4HT, dissolved in 100% ethanol as the vehicle) for 24 h (referred to as *atg7;Cre*-4HT). The control fish were treated with 100% ethanol (*atg7;Cre*-EtOH) (Fig 2A). As indicated by the cerulean fluorescence in the ventricle, the cre-mediated genomic recombination was shown to be successful 1 week after incubation with 4HT (Fig 2B and C), and an ~14-fold increase in *atg7* transcripts was seen in zebrafish cardiomyocytes (Fig 2D). As a consequence, LC3-II levels in the *atg7;Cre*-4HT zebrafish were significantly higher, and the ratio between samples treated with and without BafA1 was also higher in these zebrafish than in the *atg7*;*Cre*-EtOH zebrafish (Fig 2E and F). These data indicate effective induction of basal autophagy and autophagic flux in zebrafish with *atg7* OE, as has been noted in mouse cardiomyocytes with Atg7 OE [20]. Similar to the mice with *Atg7* OE, the zebrafish with *atg7* OE did not develop gross health issues and had normal cardiac function until they were six months of age (Fig 2H to J, the WT NS group vs *atg7;Cre*-4HT NS group). We injected a single dose of 20 mg/kg DOX into the *atg7;Cre*-4HT zebrafish seven days after administrating 4HT and then assessed ventricular function at either 1 wpi or 8 wpi via high-frequency echocardiography (Fig 2G). DOX stress induced a significant decline in EF in the adult zebrafish with *atg7 OE* 1 wpi (Fig 2H). Consistent with this observation, the activated transcript expression of *nppa* and *nppb* was increased in the DOX-treated *atg7;Cre*-4HT zebrafish 1 wpi (Fig 2I), suggesting that *atg7* OE led to deleterious effects in the aAIC model 1 wpi.

atg7 OE can reverse cardiac function decline in the late phase in the aAIC model.

In contrast to the deleterious effects observed at 1 wpi, *atg7* OE exerted salutary effects 8 wpi: the significant decline in EF in the DOX-stressed adult fish with *atg7* OE 8 wpi was reversed in the *atg7;Cre*-4HT fish (Fig 2J), as was the activated transcript expression of *nppa* and *nppb* (Online Fig II E). Because the autophagic dysregulation in the early and late phases of aAIC had opposite effects (Fig 1C to G), we reasoned that the therapeutic effects of *atg7* OE might reflect a predominant benefit in the later phase, overcoming the deleterious effects it causes during the early phase. To test this possibility, we treated *atg7;cre* adult fish with 4HT for 24 h at 4 wpi, when EF had already declined by ~12% (Fig 3A and B). Indeed, *atg7* OE was able to reverse the decline in cardiac function, as indicated by a significantly improved EF 8 wpi (Fig 3C). Consistent with this observation, the expression of activated *nppa* and *nppb* was also decreased (Fig 3D).

To determine the impact of *atg7* OE on autophagy in the context of aAIC, we measured the LC3-II protein expression level 8 wpi and its response to BafA1 treatment. Consistent with our previous study in WT fish, we noted reduced autophagy and autophagic flux in the *atg7;Cre*-EtOH upon DOX stress, both of which were effectively rescued by *atg7;Cre*-4HT

(Fig 3E and F). Together, our studies using a conditional transgenic zebrafish line revealed time-dependent effects of an autophagy-activating therapy approach that is able to reverse reduced cardiac function in the later phase of aAIC.

FDA-approved autophagy activators (FAAs) are ranked based on their therapeutic effects in an embryonic zebrafish AIC (eAIC) model.

For further translation of autophagy-based therapy, we decided to repurpose FDA-approved autophagy activating drugs. To increase the screening efficiency for assessing larger number of compounds, we turned to the eAIC model that manifests phenotypes in 3 days. After treating embryos 1 day postfertilization (dpf) with 5 different doses of DOX, [25] (Online Fig IIIA and B), we determined that the LD50 at 3 dpf was approximately 100 μmol/L, a concentration that was later used for screening. Similar to recent reports [25], the hearts of the DOX-treated zebrafish manifested pericardiac edema, elongation (n= 21/36), decreased cardiac function (n= 26/36), reduced tail vein blood flow, and reduced heart rate 3 dpf (Online Fig IIIC to F). Consistent with the therapeutic effects of mTOR inhibition in the aAIC model,[17] we noted therapeutic effects of *mtor+/−* in the eAIC model, as evident in a better survival rate, fraction shortening (FS) and heart rate (Online Fig IIIG to I). Reduced LC3-II expression (Fig 4B and C) and compromised LC3-II induction upon BafA1 treatment were noted in the eAIC model 3 dpf (Fig 4D and E), suggesting reduced basal autophagy and reduced autophagic flux. The administration of autophagy inhibitors such as BafA1 and 3-MA led to further deterioration in the eAIC model zebrafish. In contrast, the administration of autophagy activators such as rapamycin and Beclin-1 peptide exerted therapeutic effects, as indicated by rescued mortality and improved cardiac function (Fig 4F and G). Together, these data support the use of an efficient eAIC model for screening autophagy-modulating drugs.

Thirty-seven FDA-approved drugs that were previously identified as autophagy activators using an *in vitro* cell culture system were selected for further study.[26–29] We determined the LD50 for these drugs and found that 18 of the 37 tested drugs had an LD50 less than 20 μmol/L (Online Table I), a dose frequently used to conduct high-throughput screening.[30] Among the 37 drugs, digoxin, dasatinib, nitrendipine, and proscillaridin A induced teratogenic phenotypes when administered at a dose of approximately LD50 (Online Fig IV). We thus administered lower doses at 1/20, 1/40, 1/80, 1/160, and 1/320 of the LD50, aiming to identify the lowest effective dose (ED). For example, we determined that 35.92 μmol/L minoxidil was able to improve survival rates and rescue FS and heart rates (Online Fig V A to D). Based on the survival data, 21 FAAs showed significant therapeutic effects, $P<0.05$ (Fig VIA). With heart function (FS) and heart rate used as criteria, 14 and 13 FAAs had significant therapeutic effects ($P<0.05$), respectively (Online Fig VI B and C). We were able to rank these FAAs by using an arbitrary score that weighted all three indices and teratogenic effects (Fig 4H, Online Table II). Among the 18 effective FAAs, 8 were previously suggested as potential therapeutic compounds for AIC based mostly on *in vitro* models (Online Table II), while the other 10 FAAs were new drug candidates for AIC treatment.

Top-ranking FAAs from an eAIC-based screen exert therapeutic effects in both a zebrafish aAIC model and a mouse AIC model in a time-dependent fashion.

To confirm FAAs identified in the eAIC-based screening effort in the aAIC model, we assessed the following 3 drugs: pravastatin (Pra), spironolactone (Spi), and minoxidil (Mino), which ranked higher than rapamycin (Rapa); Rapa was used as a positive control; and 3-MA, an autophagy inhibitor, as a negative control. We deduced the corresponding doses in adult fish based on the effective dose (ED) that was determined experimentally in the eAIC model using a formula based on body weight ratio (Online Fig VII). We then assessed the therapeutic effects of this group of 5 drugs in the aAIC model via daily gavage for 4 weeks. Consistent with our autophagy dynamic studies and genetic studies, we noted different or opposite effects of these drugs administered in the early phase (1–4 wpi) (Fig 5A) and the late phase (4–8 wpi) (Fig 5E). Pra, Mino and Rapa administered in the early phase exerted detrimental effects, as measured by survival, and 3-MA exerted therapeutic effects, as indicated by both FS and survival (Fig 5B to D). In contrast, Pra, Mino and Rapa administered in the late phase exerted therapeutic effects, as measured by EF, FS and survival; Spi exerted therapeutic effects, as measured by EF and FS; and 3-MA exerted deleterious effects, as measured by survival (Fig 5F to H). These results confirmed the therapeutic effects of autophagy activators in the aAIC model and underscored its time-dependent nature.

Next, we sought to translate the FAAs identified from zebrafish to mammals. Several AIC models co-exist in the literature with inconsistent phenotypes, partially due to different drug delivery protocols. [31–33] We decided to follow a tail vein intravenous (IV) injection protocol that incurs minimal constitutional symptom, [12] and compare it with the intraperitoneal (IP) route. We injected 5 mg/kg DOX 4 times in succession via either the intraperitoneal (IP) route or IV route through the tail vein (Online Fig VIII A). Indeed, the mice injected via the IP route had high mortality and failed to manifest a significant reduction in EF 8 wpi (Online Fig VIII B and C), while the mice injected via the IV route had much better survival and manifested significant heart dysfunction 8 wpi (Online Fig VIII B and C). Phenotyping of the IV model revealed increased circulating levels of LDH2 and CK-MB, markers of cell and myocardial injury, respectively; increased double strand breaks (DSBs) of DNA, as indicated by g-H2AX staining; increased apoptosis, ROS activity, and fibrosis (Online Fig IX); thus, we decided to adopt the IV model for drug assessment. We did note an increased heart weight/body weight ratio; however, this is largely owing to reduced body weight (Fig 6K, Online Fig VIII D, E and G), suggesting heart weight/tibial length as a potential better index for future studies. We assessed the effects of the 4 top FAAs, Pra, Spi, Mino and Rapa, by daily gavage for 4 weeks during the early phase (1–4 wpi) (Fig 6A) or the late phase (4–8 wpi), when heart function had already declined (Fig 6E).[12] Mino and Rapa administered during the early phase exerted deleterious effects on EF, while Pra and Spi did not affect cardiac function (Fig 6B to D). On the other hand, administration of Pra, Spi, Mino and Rapa during the late phase effectively rescued cardiac dysfunction 8 wpi (Fig 6F), which can be largely ascribed to rescued LVEDD (Fig 6G and H). Consistent with the rescued cardiac function, also rescued are circulating levels of CK-MB and LDH2 (Fig 6I and J), histopathology abnormality, fibrosis, as well as mitochondria damage and vacuolization at the ultrastructural level (Online Fig X). Body weight was also significantly improved by

administration of these four FAAs (Fig 6K). None of these 4 drugs interferes with anti-tumor function of doxorubicin (Online Fig XI).

Spironolactone (Spi) and rapamycin (Rapa) activate autophagosome formation in an Atg7-dependent fashion.

In the mouse AIC model, blunted autophagic flux has been reported, which is consistent with the late phase of aAIC in our zebrafish model; however, activated autophagy in the early phase was not observed.[12, 34] We postulated that the four consecutive injections of low-dose DOX in the model mice, which differed from the single injection of high-dose DOX administered to the aAIC model zebrafish, may explain these results. To test this hypothesis, we injected a single bolus of 20 mg/kg DOX into the mice, isolated the heart, and then assessed the LC3-II expression. Indeed, we detected both activated LC3-II and an increased response to BafA1 (Fig 7A).

Because of the therapeutic effects of *atg7* OE in the late phase of the aAIC model, we reasoned that some FAAs might exert their therapeutic effects by regulating Atg7 expression. To test this hypothesis, we assessed Atg7 expression in the mouse AIC model, since an anti-Atg7 antibody is commercially available for use in this animal. We detected significantly reduced Atg7 expression 8 wpi, supporting the supposition of an important function of Atg7 in the late phase of AIC pathogenesis. Daily administration of Spi and Rapa, but not Pra or Min, restored Atg7 expression (Fig 7B). To test the hypothesis that Spi and Rapa activate autophagy by modulating Atg7 expression, we turned to an H9C2 cardiac cell line. An LC3-RFP-GFP tandem reporter construct was transfected into these cells to indicate the formation of autophagosomes and autolysosomes. We found that both Spi and Rapa induced an increase in Atg7 protein levels (Fig 7C), which sequentially activated autophagosome formation, as indicated by yellow puncta with both GFP and RFP (Fig 7D and E). Inhibition of Atg7 via co-transfection with Atg7 siRNA effectively reduced Atg7 levels and ablated the induction of autophagosomes by both Spi and Rapa (Fig 7F and G).

Top2b is required for Atg7-mediated autophagy in the early not late phase of AIC.

Finally, to understand Atg7-mediated autophagy in the context of Top2b signaling, we carried epistatic analysis between *Atg7* and *Top2b*. Similar to an increased Atg7 expression at 4 wpi and reduced expression at 8 wpi in the mouse AIC model (Fig 8A), dynamic expression was also noted in the H9C2 cell culture system, manifesting as increased Atg7 expression at 3 hour post DOX stimulation and reduced Atg7 expression at 18 hour post DOX stimulation (Fig 8C and D). Through knocking down Top2b using a Top2b siRNA (Fig 8B), we found that Top2b is required for DOX to modulate Atg7 and LC3 expression at 3 hours, but not 18 hours post DOX stimulation (Fig 8D and E). Conversely, we enquired whether Top2b expression is regulated by Atg7 by using *atg7* KO and *atg7* OE lines in zebrafish. We detected no significant changes of *top2b* transcript in both genetic manipulations (Online Fig II F). Together, these data suggested that Atg7 and Top2b pathways only interact at the early phase, when Top2b confers the primary insults imposed by DOX that sequentially activates Atg7-mediated autophagy. By contrast, reduced Atg7 expression at the late phase of AIC is independent of Top2b, representing a distinct pathological event that can be harnessed as a novel therapeutic avenue.

DISCUSSION

Cardiac dysfunction in the late phase of aAIC is reversed by *atg7*-based autophagy activation in cardiomyocytes.

As chronic AIC represents a cardiomyopathy with poor prognosis in most cases and because no mechanism-based therapy is available to treat patients in this late stage, the current work is significant, as it points towards reversal of cardiac dysfunction in the later phase of aAIC with an autophagy-activating approach. The initial insight came from our genetic studies with *Tg(βact2:atg7);Tg(cmlc2:CreER)* zebrafish, allowing for conditional overexpression of *atg7* in cardiomyocytes in a time-dependent fashion. The merit of an autophagy-activating approach was further validated by pharmacological studies of top-ranking FAAs that were identified through drug screening based on therapeutic efficacy in eAIC zebrafish model, followed by assessment and validation in both adult zebrafish and mouse models of AIC. Together, these data strongly suggest that dysregulated autophagy drives the pathophysiological momentum in the late phase of AIC and that *atg7* is a gene target that can be manipulated to exert therapeutic benefits. Using mouse and cell culture models, we found that reduced Atg7 expression is a characteristic molecular event for dysregulated autophagy in this later phase of AIC, and both Spi and Rapa activate Atg7 and are therapeutically effective. However, as Pra and Mino also exert therapeutic benefits without restoring Atg7 expression, Atg7 might not be the only target gene for autophagy-based therapy. Future studies are warranted to determine whether other autophagy genes can be manipulated to exert similar or even better therapeutic effects than realized with *atg7*.

Our conclusion on the therapeutic effects of autophagy activation is consistent with two previous pharmacological studies: In one study, rapamycin, an mTOR inhibitor, was administered to aAIC model zebrafish,[17] and in the other study, calorie restriction was combined with resveratrol to treat aAIC model rats.[13] However, our data on the accumulative long-term effects of *atg7* OE appear to contradict those from studies of *Beclin 1* OE in mice,[12] which showed deleterious effects that are similar to the short-term effects of *atg7* OE in the early phase of aAIC. On the other hand, *Beclin 1+/−*, had an attenuating effect on AIC in mice, which is consistent with the therapeutic effect of *atg7+/−* in our aAIC zebrafish model. Together with the similar autophagic flux defects in our zebrafish model and mouse AIC models reported in the literature, we reasoned that the discrepancy between *Beclin 1* OE in mice and *atg7* OE in fish is not likely due to differences in species. In contrast, the inconsistency might result from the temporal-dependent nature of autophagy dysregulation and/or the distinct functions of Atg7 and Beclin 1 in autophagy. These possibilities can be tested by temporally dependent genetic manipulations of *Beclin 1* in animal models.

Because atg7 overexpression promotes both basal autophagy and autophagic flux, we favor the statement that re-activation of the attenuated autophagy and autophagic flux in cardiomyocytes is the underlying molecular mechanism. It is likely that cardiac dysfunction in AIC is reversed because of the restored capacity of cells to remove toxic proteins and damaged organelles via autophagy, thereby improving cellular homeostasis.[9, 35] Together with the known therapeutic effects of Atg7 overexpression on pressure overload (PO)-

induced cardiac dysfunction and desmin-related cardiomyopathy, [19–21] our data on AIC raised a possibility that dysregulated autophagy is a common pathological event at the late stage of different types of heart failures, and that repairing autophagy via modulating Atg7 could be a common therapeutic strategy.

Stage-specific functions of autophagy in the early vs late phase of AIC.

Our studies converge on the important concept that pathological signaling in the late phase of AIC can be quite different from, or even opposite to, the signaling in the early phase. In the early phase of AIC in the adult models, we noted activated autophagy, salutary effects of autophagy inhibitors, and deleterious effects of *atg7* OE and autophagy activators, and all these effects were opposite those observed in the late phase. These effects were also observed in chemical-genetic studies using the mouse AIC model. In human AIC patients, initial pathological changes in the early phase represent immediate cardiac responses to anthracycline-induced damage, which might consist of excessive free radicals, iron overload, DNA damage and mitochondrial defects.[1] In most patients, this damage is either mild or repairable; thus, these patients do not develop chronic AIC. Only hearts that cannot deal with the initial damage of early AIC progress to sequential pathological changes months or years after chemotherapy. In this late phase of AIC, affected hearts manifest a different type of autophagy dysregulation than that in the early phase, contributing to the deterioration of cardiac function that ultimately leads to heart failure.

The time-dependent signaling hypothesis of AIC helps to explain why both *atg7+/−* and *atg7* OE exerts accumulative therapeutic effects in the aAIC model. Based on our experimental evidence, *atg7* OE exerts a deleterious effect in the early phase but a salutary effect in the later phase. Thus, we conclude that the accumulative therapeutic effect of *atg7* OE is due to the combination of a weak deleterious effect in the early phase and a strong therapeutic effect in the late phase. Similarly, we reasoned that the accumulative therapeutic effects of *atg7+/−* can be explained by a combination of strong cardioprotective effects in the early phase and no or mild deleterious effect in the later phase. Definitive evidence for the latter prediction can be obtained by generating a conditional *atg7*-KO line for time-dependent genetic manipulation.

Our time-dependent signaling hypothesis needs to be considered when developing mechanism-based therapies for AIC. Different types of therapeutic strategies must be tailored to treat the early phase and late phase of AIC, respectively. Most research efforts in this area have focused on the initial damage incurred by DOX and the repair of this damage. However, caution is advised when pursuing this strategy considering a recent study on p53.[36] While the inhibition of p53 exhibited a therapeutic effect within the first week after DOX injection, AIC phenotypes were exacerbated 13 weeks after DOX injection.[37] Thus, an antidote is only effective when administered at the right time with the right dose; otherwise, it can be a toxin.

A zebrafish-mouse drug assessment platform accelerates the repositioning of FDA-approved drugs to treat AIC.

Given that the development of a drug typically takes more than 10 years and costs more than 1 billion dollars, repurposing existing FDA-approved drugs is an appealing strategy. While it is a daunting task to screen a large number of candidate drugs directly using a mouse AIC model, the small body size and the low maintenance costs of zebrafish enable a much more efficient approach on a larger scale. Here, we present an embryonic zebrafish to adult zebrafish to mouse drug screening platform for rapid assessment of AIC treatment compounds based on their therapeutic efficacy. The successful integration of the eAIC model enables this platform to be useful for screening thousands of compounds,[15, 38] thereby eliminating poor performers and ensuring that only top-ranking compounds are tested in the zebrafish aAIC and mouse AIC models. We fully expect that our platform will be extended to screening compounds in other signaling pathways, accelerating drug discovery for AIC.

Using an eAIC model to assess the therapeutic efficacy of drugs for late phase aAIC is counterintuitive because of the assumption that an eAIC model would recapitulate the acute damage incurred by DOX. However, the strategy is supported by coherent findings of autophagic flux defects, therapeutic effects of autophagy activators, and deleterious effects of autophagy inhibitors in both eAIC and late phase aAIC. It is possible that both early phase and late phase effects manifest in the eAIC model, with the late phase effect playing a more predominant role.

Spironolactone, acting through competitive binding of receptors at the aldosterone-dependent sodium-potassium exchange site in the distal convoluted renal tubule, is currently used clinically as a diuretic drug, antihypertensive treatment, and an aldosterone antagonist in patients with heart failure. Pravastatin has been used to reduce hypercholesterolemia and the risk of cardiovascular events. Here, our pharmacological studies in both zebrafish and mice suggest therapeutic effects of these drugs on AIC via autophagy activation. As a future direction, these drugs should be further tested in large mammals and/or in human clinical trials with the aim of translating our discovery to reverse cardiac dysfunction in AIC patients.

In summary, this work established autophagy-based therapy as the first mechanism-based therapeutic avenue that can lead to a reversal of AIC in patients after their cardiac function has deteriorated. Compared to therapies targeting the early phase, such as Top2b-based therapy, that need to preventatively treat all chemotherapy patients, therapies directed to late phase AIC are administered only to a subpopulation of patients who manifest chronic cardiac phenotypes. Superior to therapies targeting the early phase that need to ensure minimal interference with the anticancer functions of DOX, this new type of therapeutic strategy bypasses this requirement because of differences in the treatment time windows. It is highly anticipated that more mechanism-based therapies targeting the late phase of AIC will be developed and that an efficient zebrafish model will accelerate the discovery process.

Supplementary Material

Refer to Web version on PubMed Central for supplementary material.

ACKNOWLEDGMENTS

We thank Beninio Gores and Kashia Stragey for managing the zebrafish facility.

SOURCES OF FUNDING

This study was supported by grants from the Mayo Foundation and Mayo Clinic Center for Biomedical Discovery (CBD) — Cardiovascular Research Center Award (grant no. FP00105557) to X.X. and J.H. and a Major New Drug Discovery award from the Ministry of Science and Technology, China (grant no. 2019ZX09201004-001-011) to Y.W.. X. L. is funded by the China Scholarship Council.

Nonstandard Abbreviations and Acronyms:

AIC
Anthracycline-induced cardiotoxicity

aAIC
adult Anthracycline-induced cardiotoxicity

BafA1
bafilomycin A1

CYP1
cytochrome P450 family 1

CMC
carboxymethylcellulose

CK-MB
creatine kinase-MB

DOX
doxorubicin

dpi
day post-injection

DMSO
dimethyl sulfoxide

DHE
Dihydroethidium

DBS
double strand breaks

ED
effective dose

EF
ejection fraction

eAIC
Embryonic Anthracycline-induced cardiotoxicity

FDA
Food and Drug Administration

FAA
FDA-approved autophagy activator

FS
fraction shortening

HE
Hematoxylin and eosin

HF
heart failure

IV
intravenous

LDH
lactate dehydrogenase

LVEDD
left ventricular end-diastolic dimension

LVESD
eft ventricular end-systolic dimension

Mino
minoxidil

nppa
natriuretic peptide A

nppb
natriuretic peptide B

OE
overexpression

Pra
pravastatin

Rapa
rapamycin

Spi
spironolactone

Top 2b
Topoisomerase 2b

TEM
Transmission electron microscopy

wpi
weeks post injection

WT
wild type

ZIRC
Zebrafish International Resource Center

4HT
4-hydroxytamoxifen

REFERENCES

1. Herrmann JAdverse cardiac effects of cancer therapies: cardiotoxicity and arrhythmia. Nat Rev Cardiol. 2020;17:474–502. [PubMed: 32231332]
2. Zamorano JL, Lancellotti P, Rodriguez Munoz D, Aboyans V, Asteggiano R, Galderisi M, Habib G, Lenihan DJ, Lip GYH, Lyon AR, Lopez Fernandez T, Mohty D, Piepoli MF, Tamargo J, Torbicki A, Suter TM and Group ESCSD. 2016 ESC Position Paper on cancer treatments and cardiovascular toxicity developed under the auspices of the ESC Committee for Practice Guidelines: The Task Force for cancer treatments and cardiovascular toxicity of the European Society of Cardiology (ESC). Eur Heart J. 2016;37:2768–2801. [PubMed: 27567406]
3. Nadruz W, Jr., West E, Sengelov M, Grove GL, Santos M, Groarke JD, Forman DE, Claggett B, Skali H, Nohria A and Shah AM. Cardiovascular phenotype and prognosis of patients with heart failure induced by cancer therapy. Heart. 2019;105:34–41. [PubMed: 29764969]
4. FELKER RET GM, HARE JM, HRUBAN RH, CLEMETSON DE, HOWARD DL, BAUGHMAN KL, AND KASPER EK. Underlying causes and long-term survival in patients with initially unexplaine cardiomyopathy. The New England Journal of Medicine. 2000;342:1077–1084. [PubMed: 10760308]
5. Vejpongsa P and Yeh ET. Prevention of anthracycline-induced cardiotoxicity: challenges and opportunities. J Am Coll Cardiol. 2014;64:938–45. [PubMed: 25169180]
6. Zhang S, Liu X, Bawa-Khalfe T, Lu LS, Lyu YL, Liu LF and Yeh ET. Identification of the molecular basis of doxorubicin-induced cardiotoxicity. Nat Med. 2012;18:1639–42. [PubMed: 23104132]
7. Deng S YT, Jendrny C, Nemecek A, Vincetic M, Gödtel-Armbrust U, Wojnowski L. Dexrazoxane may prevent doxorubicin-induced DNA damage via depleting both topoisomerase II isoforms. BMC Cancer. 2014;14. [PubMed: 24410891]
8. Yeh ET and Chang HM. Oncocardiology-Past, Present, and Future: A Review. JAMA Cardiol. 2016;1:1066–1072. [PubMed: 27541948]
9. Sciarretta S, Maejima Y, Zablocki D and Sadoshima J. The Role of Autophagy in the Heart. Annu Rev Physiol. 2018;80:1–26. [PubMed: 29068766]
10. Zech ATL, Singh SR, Schlossarek S and Carrier L. Autophagy in cardiomyopathies. Biochim Biophys Acta Mol Cell Res. 2020;1867:118432. [PubMed: 30831130]

11. Bartlett JJ, Trivedi PC, Yeung P, Kienesberger PC and Pulinilkunnil T. Doxorubicin impairs cardiomyocyte viability by suppressing transcription factor EB expression and disrupting autophagy. Biochem J. 2016;473:3769–3789. [PubMed: 27487838]
12. Li DL, Wang ZV, Ding G, Tan W, Luo X, Criollo A, Xie M, Jiang N, May H, Kyrychenko V, Schneider JW, Gillette TG and Hill JA. Doxorubicin Blocks Cardiomyocyte Autophagic Flux by Inhibiting Lysosome Acidification. Circulation. 2016;133:1668–87. [PubMed: 26984939]
13. Dutta D, Xu J, Dirain ML and Leeuwenburgh C. Calorie restriction combined with resveratrol induces autophagy and protects 26-month-old rat hearts from doxorubicin-induced toxicity. Free Radic Biol Med. 2014;74:252–62. [PubMed: 24975655]
14. Asnani A, Zheng B, Liu Y, Wang Y, Chen HH, Vohra A, Chi A, Cornella-Taracido I, Wang H, Johns DG, Sosnovik DE and Peterson RT. Highly potent visnagin derivatives inhibit Cyp1 and prevent doxorubicin cardiotoxicity. JCI Insight. 2018;3.
15. Liu Y, Asnani A, Zou L, Bentley VL, Yu M, Wang Y, Dellaire G, Sarkar KS, Dai M, Chen HH, Sosnovik DE, Shin JT, Haber DA, Berman JN, Chao W and Peterson RT. Visnagin protects against doxorubicin-induced cardiomyopathy through modulation of mitochondrial malate dehydrogenase. Sci Transl Med. 2014;6:266ra170.
16. Ma X, Ding Y, Wang Y and Xu X. A Doxorubicin-induced Cardiomyopathy Model in Adult Zebrafish. J Vis Exp. 2018.
17. Ding Y, Sun X, Huang W, Hoage T, Redfield M, Kushwaha S, Sivasubbu S, Lin X, Ekker S and Xu X. Haploinsufficiency of target of rapamycin attenuates cardiomyopathies in adult zebrafish. Circ Res. 2011;109:658–69. [PubMed: 21757652]
18. Noda NN, Satoo K, Fujioka Y, Kumeta H, Ogura K, Nakatogawa H, Ohsumi Y and Inagaki F. Structural basis of Atg8 activation by a homodimeric E1, Atg7. Mol Cell. 2011;44:462–75. [PubMed: 22055191]
19. Qi L, Zang H, Wu W, Nagarkatti P, Nagarkatti M, Liu Q, Robbins J, Wang X and Cui T. CYLD exaggerates pressure overload-induced cardiomyopathy via suppressing autolysosome efflux in cardiomyocytes. J Mol Cell Cardiol. 2020;145:59–73. [PubMed: 32553594]
20. Bhuiyan MS, Pattison JS, Osinska H, James J, Gulick J, McLendon PM, Hill JA, Sadoshima J and Robbins J. Enhanced autophagy ameliorates cardiac proteinopathy. J Clin Invest. 2013;123:5284–97. [PubMed: 24177425]
21. Pattison JS, Osinska H and Robbins J. Atg7 induces basal autophagy and rescues autophagic deficiency in CryABR120G cardiomyocytes. Circ Res. 2011;109:151–60. [PubMed: 21617129]
22. Busch-Nentwich E, Kettleborough R, Dooley CM, Scahill C, Sealy I, White R, Herd C, Mehroke S, Wali N, Carruthers S, Hall A, Collins J, Gibbons R, Pusztai Z, Clark R, and Stemple DLSanger Institute Zebrafish Mutation Project mutant data submission. . 2013.
23. Lee E, Koo Y, Ng A, Wei Y, Luby-Phelps K, Juraszek A, Xavier RJ, Cleaver O, Levine B and Amatruda JF. Autophagy is essential for cardiac morphogenesis during vertebrate development. Autophagy. 2014;10:572–87. [PubMed: 24441423]
24. Mawed SA, Zhang J, Ren F and Mei J. Autophagy-related genes atg7 and beclin1 are essential for energy metabolism and survival during the larval-to-juvenile transition stage of zebrafish. bioRxiv. 2019:666883.
25. Robertson AL, Holmes GR, Bojarczuk AN, Burgon J, Loynes CA, Chimen M, Sawtell AK, Hamza B, Willson J, Walmsley SR, Anderson SR, Coles MC, Farrow SN, Solari R, Jones S, Prince LR, Irimia D, Rainger GE, Kadirkamanathan V, Whyte MK and Renshaw SA. A zebrafish compound screen reveals modulation of neutrophil reverse migration as an anti-inflammatory mechanism. Sci Transl Med. 2014;6:225ra29.
26. Levine B, Packer M and Codogno P. Development of autophagy inducers in clinical medicine. J Clin Invest. 2015;125:14–24. [PubMed: 25654546]
27. Williams A, Sarkar S, Cuddon P, Ttofi EK, Saiki S, Siddiqi FH, Jahreiss L, Fleming A, Pask D, Goldsmith P, O'Kane CJ, Floto RA and Rubinsztein DC. Novel targets for Huntington's disease in an mTOR-independent autophagy pathway. Nat Chem Biol. 2008;4:295–305. [PubMed: 18391949]

28. Hundeshagen P, Hamacher-Brady A, Eils R and Brady NR. Concurrent detection of autolysosome formation and lysosomal degradation by flow cytometry in a high-content screen for inducers of autophagy. BMC Biol. 2011;9:38. [PubMed: 21635740]
29. Zhang LYJ, Pan H, Hu P, Hao Y, Cai W, Zhu H, Yu AD, Xie X, Ma D, Yuan J. . Small molecule regulators of autophagy identified by an image-based high-throughput screen. Proc Natl Acad Sci U S A2007;104:19023–8. [PubMed: 18024584]
30. Wiley DS, Redfield SE and Zon LI. Chemical screening in zebrafish for novel biological and therapeutic discovery. Methods Cell Biol. 2017;138:651–679. [PubMed: 28129862]
31. Zhang Y, Kang YM, Tian C, Zeng Y, Jia LX, Ma X, Du J and Li HH. Overexpression of Nrdp1 in the heart exacerbates doxorubicin-induced cardiac dysfunction in mice. PLoS One. 2011;6:e21104. [PubMed: 21738612]
32. Kawaguchi T, Takemura G, Kanamori H, Takeyama T, Watanabe T, Morishita K, Ogino A, Tsujimoto A, Goto K, Maruyama R, Kawasaki M, Mikami A, Fujiwara T, Fujiwara H and Minatoguchi S. Prior starvation mitigates acute doxorubicin cardiotoxicity through restoration of autophagy in affected cardiomyocytes. Cardiovasc Res. 2012;96:456–65. [PubMed: 22952253]
33. Li M, Sala V, De Santis MC, Cimino J, Cappello P, Pianca N, Di Bona A, Margaria JP, Martini M, Lazzarini E, Pirozzi F, Rossi L, Franco I, Bornbaum J, Heger J, Rohrbach S, Perino A, Tocchetti CG, Lima BHF, Teixeira MM, Porporato PE, Schulz R, Angelini A, Sandri M, Ameri P, Sciarretta S, Lima-Junior RCP, Mongillo M, Zaglia T, Morello F, Novelli F, Hirsch E and Ghigo A. Phosphoinositide 3-Kinase Gamma Inhibition Protects From Anthracycline Cardiotoxicity and Reduces Tumor Growth. Circulation. 2018;138:696–711. [PubMed: 29348263]
34. Abdullah CS, Alam S, Aishwarya R, Miriyala S, Bhuiyan MAN, Panchatcharam M, Pattillo CB, Orr AW, Sadoshima J, Hill JA and Bhuiyan MS. Doxorubicin-induced cardiomyopathy associated with inhibition of autophagic degradation process and defects in mitochondrial respiration. Sci Rep. 2019;9:2002. [PubMed: 30765730]
35. Lavandero S, Chiong M, Rothermel BA and Hill JA. Autophagy in cardiovascular biology. J Clin Invest. 2015;125:55–64. [PubMed: 25654551]
36. McSweeney KM, Bozza WP, Alterovitz WL and Zhang B. Transcriptomic profiling reveals p53 as a key regulator of doxorubicin-induced cardiotoxicity. Cell Death Discov. 2019;5:102. [PubMed: 31231550]
37. Zhu W, Zhang W, Shou W and Field LJ. P53 inhibition exacerbates late-stage anthracycline cardiotoxicity. Cardiovasc Res. 2014;103:81–9. [PubMed: 24812279]
38. Zon LI and Peterson RT. In vivo drug discovery in the zebrafish. Nat Rev Drug Discov. 2005;4:35–44. [PubMed: 15688071]
39. S R Jones SC, Harrison M. Introduction to power analysis. Emerg Med J2003;20:453–458. [PubMed: 12954688]
40. Lenth RV. Power Analysis for Experimental Research: A Practical Guide For The Biological, Medical and Social Sciences and Statistical Power Analysis: A Simple and General Model for Traditional and Modern Hypothesis Tests. Journal of the American Statistical Association. 2004.
41. Hoage T, Ding Y and Xu X. Quantifying cardiac functions in embryonic and adult zebrafish. Methods Mol Biol. 2012;843:11–20. [PubMed: 22222517]
42. Shin JT, Pomerantsev EV, Mably JD and MacRae CA. High-resolution cardiovascular function confirms functional orthology of myocardial contractility pathways in zebrafish. Physiol Genomics. 2010;42:300–9. [PubMed: 20388839]
43. Wang LW, Huttner IG, Santiago CF, Kesteven SH, Yu ZY, Feneley MP and Fatkin D. Standardized echocardiographic assessment of cardiac function in normal adult zebrafish and heart disease models. Dis Model Mech. 2017;10:63–76. [PubMed: 28067629]
44. Ma X, Zhu P, Ding Y, Zhang H, Qiu Q, Dvornikov AV, Wang Z, Kim M, Wang Y, Lowerison M, Yu Y, Norton N, Herrmann J, Ekker SC, Hsiai TK, Lin X and Xu X. Retinoid X receptor alpha is a spatiotemporally predominant therapeutic target for anthracycline-induced cardiotoxicity. Science Advances. 2020;6:eaay2939. [PubMed: 32064346]
45. Pinzon-Olejua A WC, Chekuru A, Bosak V, Brand M, Hans S, Stuermer CA. . Cre-inducible Site-specific Recombination in Zebrafish Oligodendrocytes. DEVELOPMENTAL DYNAMICS. 2017;246:41–49. [PubMed: 27666728]

46. Gupta V, Gemberling M, Karra R, Rosenfeld GE, Evans T and Poss KD. An injury-responsive gata4 program shapes the zebrafish cardiac ventricle. Curr Biol. 2013;23:1221–7. [PubMed: 23791730]
47. Shoji-Kawata S, Sumpter R, Leveno M, Campbell GR, Zou Z, Kinch L, Wilkins AD, Sun Q, Pallauf K, MacDuff D, Huerta C, Virgin HW, Helms JB, Eerland R, Tooze SA, Xavier R, Lenschow DJ, Yamamoto A, King D, Lichtarge O, Grishin NV, Spector SA, Kaloyanova DV and Levine B. Identification of a candidate therapeutic autophagy-inducing peptide. Nature. 2013;494:201–6. [PubMed: 23364696]
48. Mathai BJ, Meijer AH and Simonsen A. Studying Autophagy in Zebrafish. Cells. 2017;6:21.
49. Thompson TN. Safety Testing of Drug Metabolites. Annual Reports in Medicinal Chemistry. 2009;44:459–474.
50. Collymore C, Rasmussen S and Tolwani RJ. Gavaging adult zebrafish. Journal of Visualized Experiments Jove, 2013(78).
51. Dang M, Henderson RE, Garraway LA and Zon LI. Long-term drug administration in the adult zebrafish using oral gavage for cancer preclinical studies. Dis Model Mech. 2016;9:811–20. [PubMed: 27482819]
52. Turner PVBT, Pekow C, Vasbinder MA. Administration of Substances to Laboratory Animals Routes of Administration and Factors to Consider. J Am Assoc Lab Anim Sci2011;50:600–613. [PubMed: 22330705]
53. Sakurabayashi-Kitade S, Aoka Y, Nagashima H, Kasanuki H, Hagiwara N and Kawana M. Aldosterone blockade by Spironolactone improves the hypertensive vascular hypertrophy and remodeling in angiotensin II overproducing transgenic mice. Atherosclerosis. 2009;206:54–60. [PubMed: 19327775]
54. Wang X, Li C, Wang Q, Li W, Guo D, Zhang X, Shao M, Chen X, Ma L, Zhang Q, Wang W and Wang Y. Tanshinone IIA Restores Dynamic Balance of Autophagosome/Autolysosome in Doxorubicin-Induced Cardiotoxicity via Targeting Beclin1/LAMP1. Cancers (Basel). 2019;11.
55. Wang X, Wang Q, Li W, Zhang Q, Jiang Y, Guo D, Sun X, Lu W, Li C and Wang Y. TFEB-NF-kappaB inflammatory signaling axis: a novel therapeutic pathway of Dihydrotanshinone I in doxorubicin-induced cardiotoxicity. J Exp Clin Cancer Res. 2020;39:93. [PubMed: 32448281]
56. Matias M SS, Falcão A, Alves G. Considerations and Pitfalls in Selecting the Drug Vehicles for Evaluation of New Drug Candidates: Focus on in vivo Pharmaco-Toxicological Assays Based on the Rotarod Performance Test. J Pharm Pharm Sci. 2018;21:110–118. [PubMed: 29543586]
57. Liu G, Liu Y, Wang R, Hou T, Chen C, Zheng S and Dong Z. Spironolactone Attenuates Doxorubicin-induced Cardiotoxicity in Rats. Cardiovasc Ther. 2016;34:216–24. [PubMed: 27097055]
58. Rita Z, Attila C, Andras C, Andrea G, Dora P, Istvan L and Arpad T. The Cardioprotective Effect of Metformin in Doxorubicin-Induced Cardiotoxicity: The Role of Autophagy. Molecules. 2018;23(5):1184.
59. Wang Y, Ma Q, Zhang S, Liu H, Zhao B, Du B, Wang W, Lin P, Zhang Z, Zhong Y and Kong D. Digoxin Enhances the Anticancer Effect on Non-Small Cell Lung Cancer While Reducing the Cardiotoxicity of Adriamycin. Front Pharmacol. 2020;11:186. [PubMed: 32180730]
60. Yu X, Ruan Y, Huang X, Dou L, Lan M, Cui J, Chen B, Gong H, Wang Q, Yan M, Sun S, Qiu Q, Zhang X, Man Y, Tang W, Li J and Shen T. Dexrazoxane ameliorates doxorubicin-induced cardiotoxicity by inhibiting both apoptosis and necroptosis in cardiomyocytes. Biochem Biophys Res Commun. 2020;523:140–146. [PubMed: 31837803]
61. Yasunori Sato NS, Megu Saito, Nao Endo, Fumihiko Kugawa, and Akemichi Ueno. Luteolin Attenuates Doxorubicin-Induced Cytotoxicity to MCF-7 Human Breast Cancer Cells. Biological and Pharmaceutical Bulletin. 2015;38:703–709 [PubMed: 25947916]
62. Dong Q, Chen L, Lu Q, Sharma S, Li L, Morimoto S and Wang G. Quercetin attenuates doxorubicin cardiotoxicity by modulating Bmi-1 expression. Br J Pharmacol. 2014;171:4440–54. [PubMed: 24902966]

NOVELTY AND SIGNIFICANCE

What Is Known?

- Anthracycline-induced cardiotoxicity (AIC) is caused by initial damage incurred by anthracyclines in the heart during chemotherapy, which results in reduced cardiac function months or years post chemotherapy.
- Autophagy dysregulation is an important pathological event that could be leveraged for therapeutic benefits for AIC.

What New Information Does This Article Contribute?

- There is a biphasic response in autophagy dysregulation - activation in the early phase and suppression in the later phase when cardiac function deteriorates.
- *atg7*-based autophagy activation in cardiomyocytes exerts therapeutic effects in the late phase, but deleterious effects in the early phase of AIC.
- A zebrafish-mouse drug assessment platform has been established to identify top FDA-approved autophagy activating drugs to treat the late phase AIC.

The utility of anthracyclines as chemotherapeutics is compromised by their dose-dependent cardiotoxicity. No effective drug is available to reverse chronic AIC when cardiac function has already deteriorated. Here, the authors carried longitudinal studies of autophagy and found that autophagy dysregulation in the late phase of AIC is different from its early phase. In consistent to this observation, Atg7-based autophagy activation exerts therapeutic effects only in the late phase, but detrimental effects in the early phase. The time-dependent nature of the autophagy-based therapy was confirmed pharmacologically by administering autophagy activators in both zebrafish and mouse AIC models. Together, the work raised an important new concept that pathological signaling in the late phase of AIC can be quite different from, or even opposite to, the signaling in the early phase. Therefore, time-dependent therapies are needed. Specifically, an autophagy-based therapy has been established as the first mechanism-based therapeutic avenue that can benefit AIC patients after their cardiac function has deteriorated. Several FDA-approved autophagy activating drugs including spironolactone and pravastatin have been identified using a zebrafish-mouse drug screen platform, which could be translated into human AIC patients.

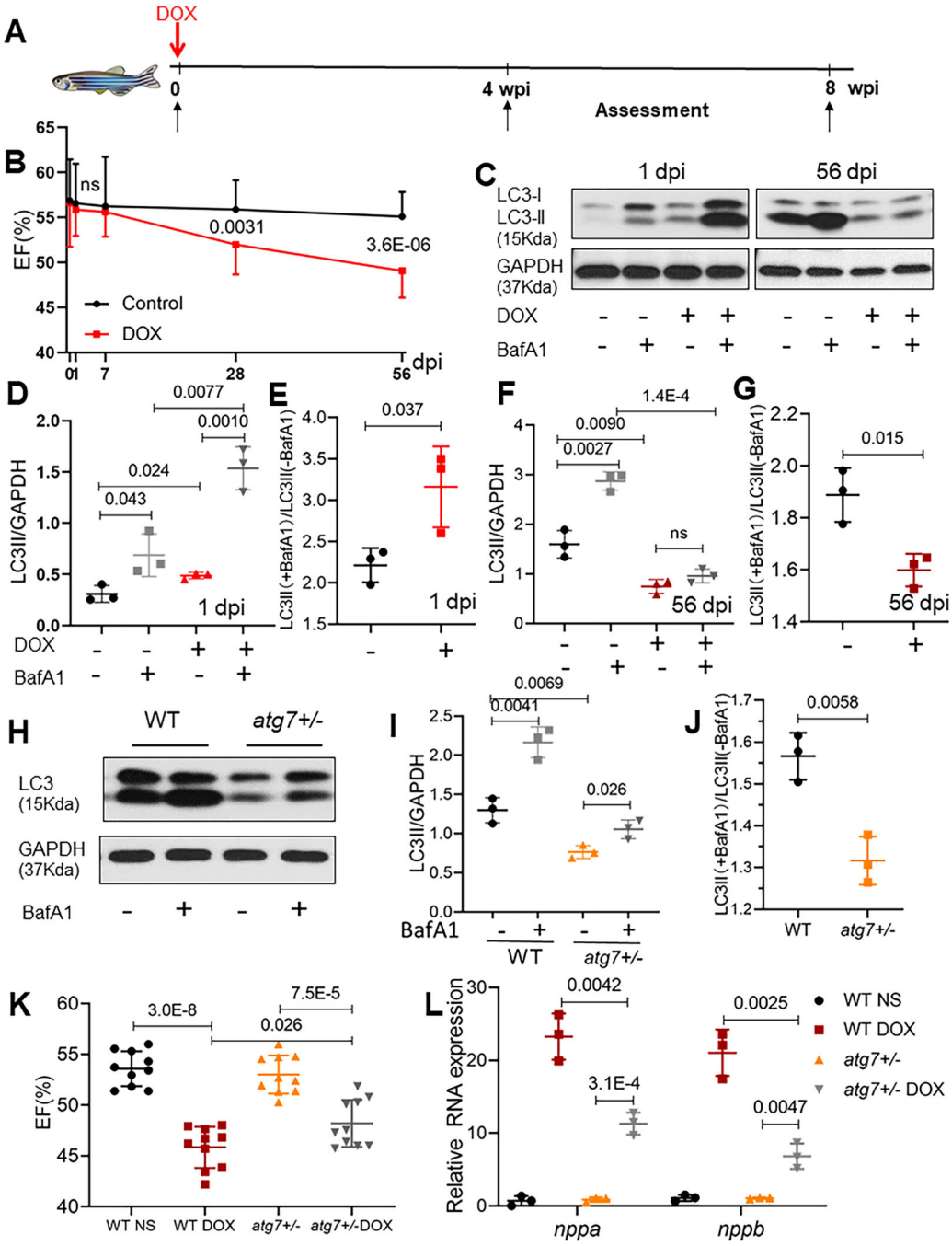

Fig 1. Dynamic autophagy signaling in a zebrafish adult AIC (aAIC) model and modifying effects of *atg7*+/−.

(A) Schematics of the experimental procedure of an anthracycline-induced cardiotoxicity (AIC) in an adult (aAIC) zebrafish model (DOX, doxorubicin). (B) Dynamics of EF% in the DOX-treated zebrafish and the control group using a high-frequency echo system (n=15). (C) Representative Western blot showing temporal changes in LC3-II protein expression in the hearts of adult zebrafish with AIC. Bafilomycin A1 (30 nM) was administered 4 h before the zebrafish were sacrificed. (D to G) Quantification of LC3-II and the ratio between hearts treated with and without BafA1 in (C), n=3 hearts/group. (H) Representative images of a

Western blot showing the LC3 expression in the hearts of WT and *atg7+/−* zebrafish in the absence or presence of 30 nM BafA1 for 4 h. (I) and (J) Quantification of the Western blot data in (H), n = 3 in each group. (K) Ventricular ejection fraction of WT and *atg7−/+* zebrafish with or without DOX stress 8 weeks post injection (wpi) (n=10 fish/group). (L) Quantification of *nppa* and *nppb* gene expression by quantitative RT-PCR. n=3 per group. Student's t test was used in (B); Mann-Whitney test in (E), (G) and (J); Kruskal-Wallis test in (D), (F), (I), and (L); one-way ANOVA followed by post hoc Tukey's test in (K).

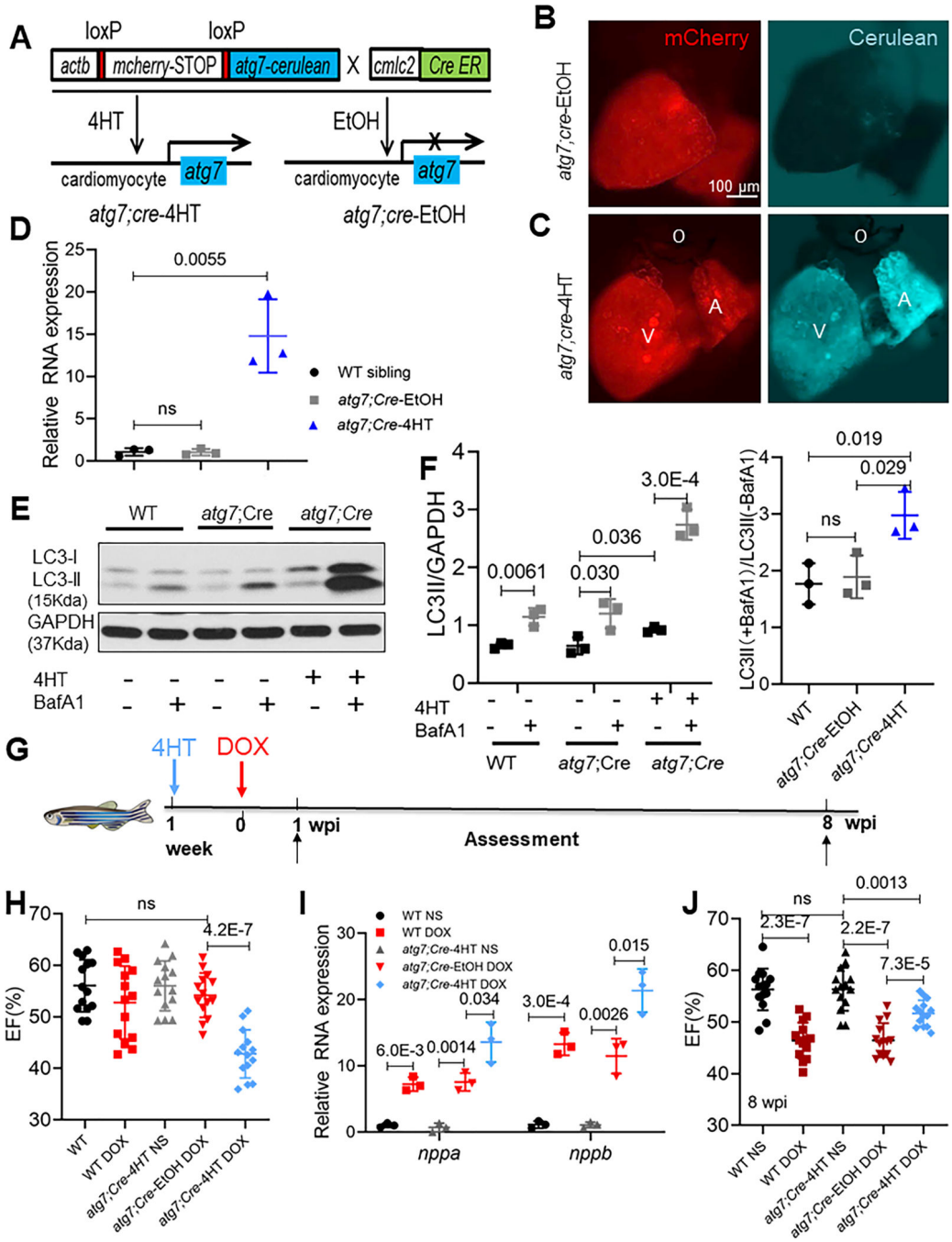

Fig 2. *atg7* overexpression (OE) activates autophagy and exerts deleterious effects in the early phase of aAIC.

(A) Schematics of the *atg7* conditional transgenic line. (B and C) Fluorescence images of hearts in fish at 1 week after 24-h treatment with 4HT or EtOH. Signals in the cerulean channel represent cardiomyocyte-specific *atg7* overexpression after conditional gene activation. (D) Relative transcript level of *atg7* RNA in a wild-type sibling and zebrafish with *atg7* OE and with and without 4HT treatment. (E) Representative Western blot showing increased LC3-II levels in a zebrafish with *atg7* OE and control treated with BafA1 (n=3/treatment). (F) Quantification of LC3-II and the ratio of LC3-II between the

hearts treated with and without BafA1 in (E). (G) Schematics of the experimental procedure for activating *atg7* in the early phase of aAIC. (H and J) High-frequency echocardiography was performed at the indicated times to quantify cardiac function. One-way ANOVA followed by Tukey's post hoc test was used. (I) Evaluation of *nppa* and *nppb* gene transcript expression by quantitative RT-PCR. (n = 3). Kruskal-Wallis test was used followed by post hoc Tukey's test in in (D), (F) and (I). WT, wild type; DOX, doxorubicin.

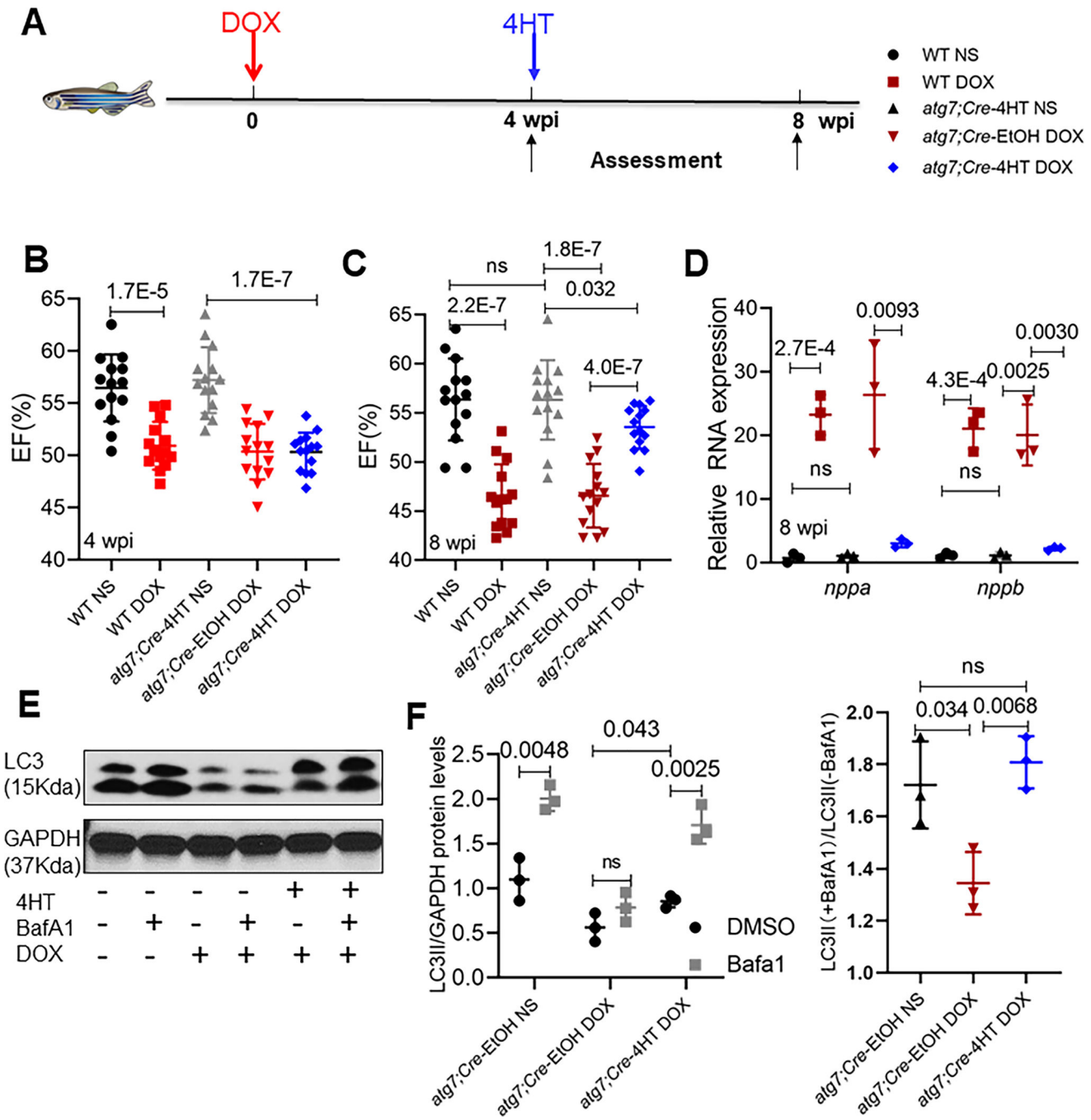

Fig 3. atg7 OE can reverse the decline in cardiac function in the late phase of aAIC.

(A) Schematics of the experimental schedule for activating *atg7* in the late phase of aAIC. (B and C) High-frequency echocardiography was performed at the indicated times to quantify cardiac function. (WT, wild type; DOX, doxorubicin) (n=15). We used bright red to represent data at the early AIC phase; dark red to represent data at the late AIC phase. One-way ANOVA followed by post hoc Tukey's test was used. (D) Evaluation of *nppa* and *nppb* gene transcript expression by quantitative RT-PCR. (n = 3). (E) Western blotting was used to assess autophagy activity in *atg7*;Cre fish hearts injected with DOX with or without

4HT treatment, as indicated by LC3-II expression. (F) Quantification of LC3-II and the ratio of LC3-II between the hearts treated with and without BafA1 in (E). (n = 3). Kruskal-Wallis test was used followed by post hoc Tukey's test in (D) and (F).

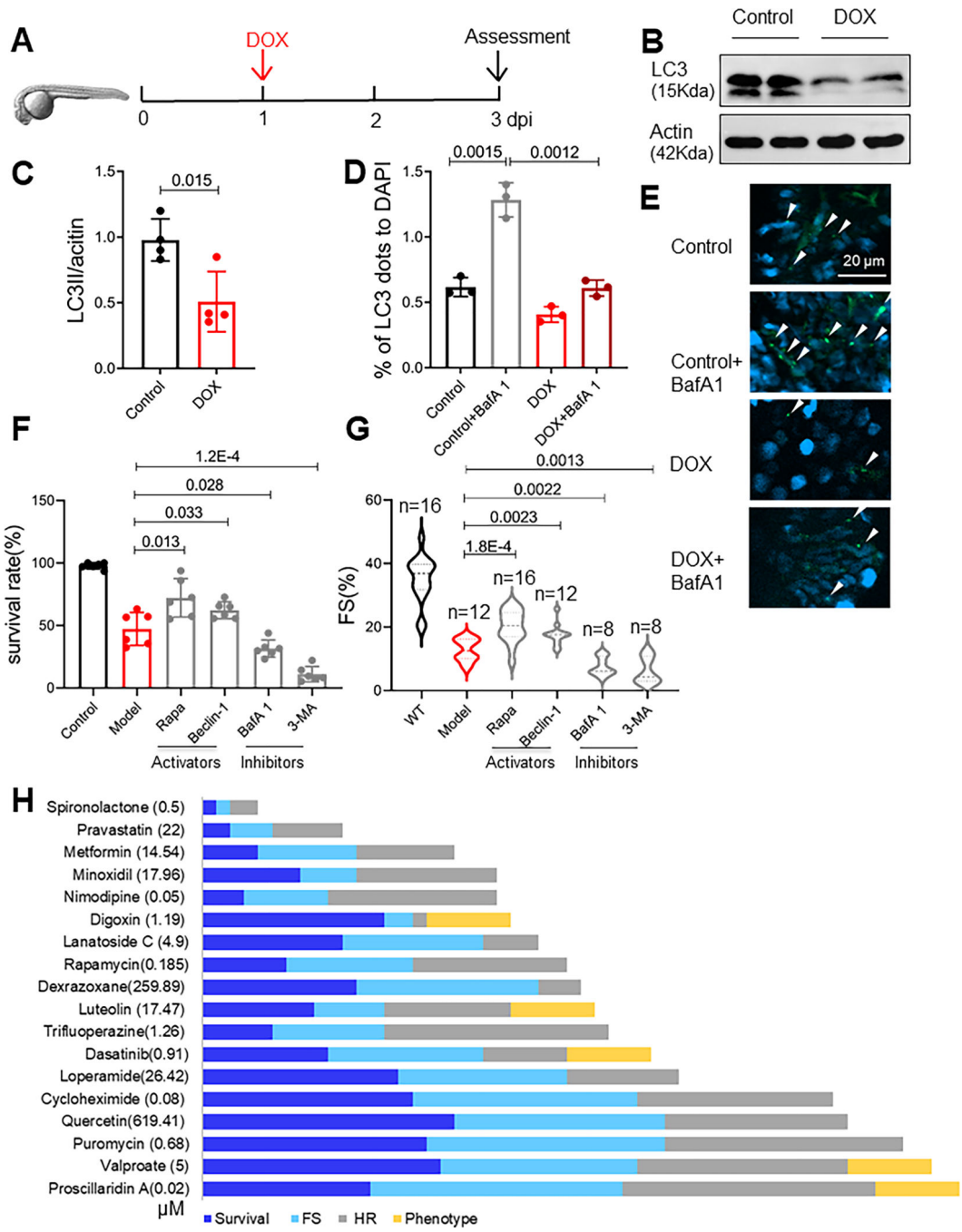

Fig 4. FDA-approved autophagy activators (FAAs) were ranked based on their therapeutic effects in a zebrafish embryonic AIC (eAIC) model.

(A) Schematics of the experimental procedure for an embryonic AIC (eAIC) model. (B and C) Representative Western blot of LC3-II in eAIC and LC3-II quantification (n=4/group). (D and E) *Tg(GFP-LC3)* zebrafish were used to quantify LC3-II induction. Arrows indicate LC3 aggregates. (n=3/group). (F and G) Autophagy activators exert therapeutic effects, and autophagy inhibitors exert detrimental effects on eAIC, as indicated by changes in both mortality and cardiac function. (H) The rank of the top 18 FAA drugs based on a composite score of their therapeutic effects based on survival rate, heart rate, heart function and

phenotypes. Mann-Whitney test in (C); Kruskal-Wallis test followed by post hoc Tukey's test in (D), (F) and (G); Kruskal-Wallis test followed by Bonferroni post hoc test in (G).

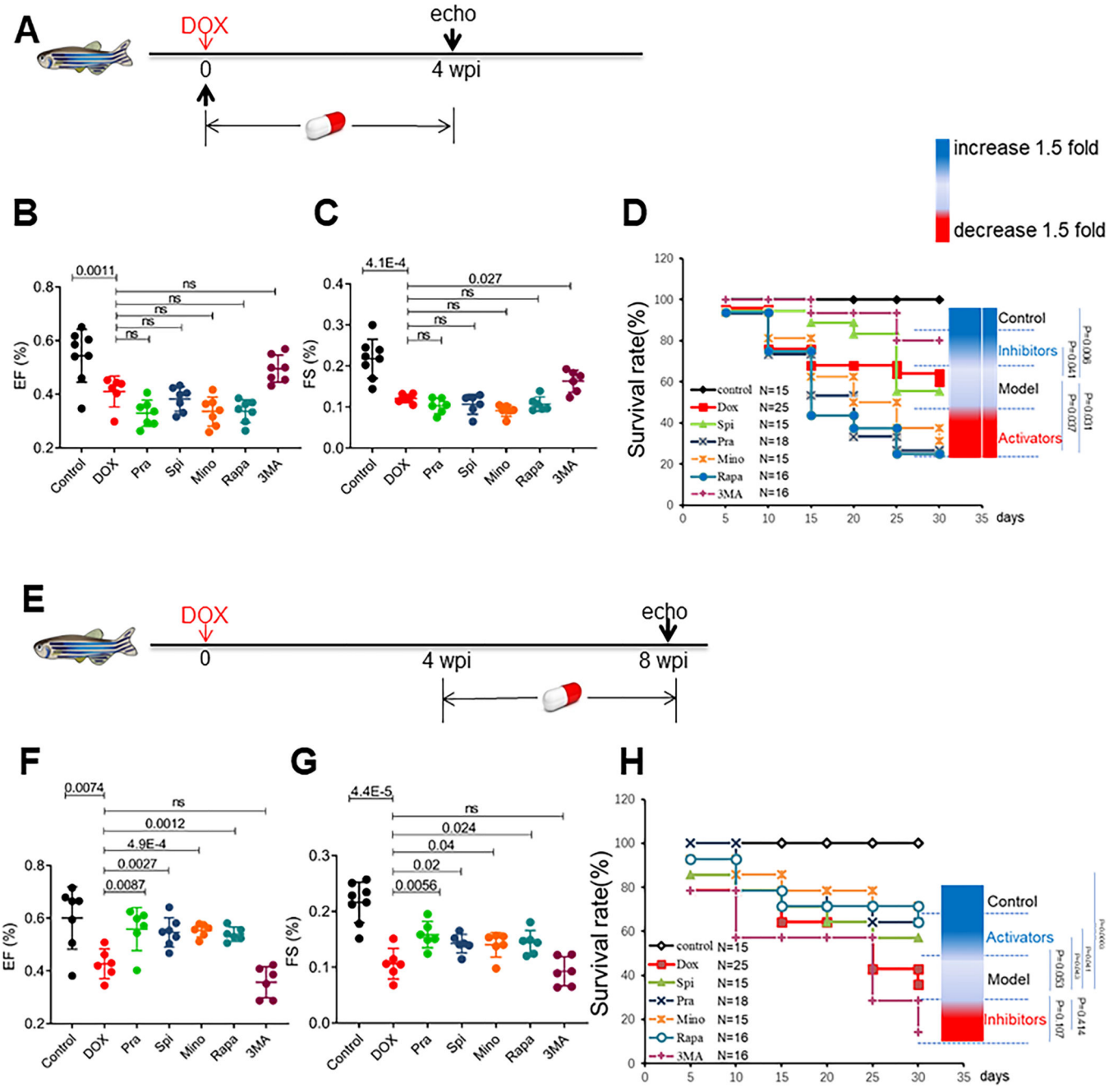

Fig 5. Top-ranking FAAs used with the eAIC model exerted therapeutic effects in the zebrafish aAIC model in a time-dependent fashion.

(A) Schematics of the experimental procedure for drug administration in the early phase of aAIC. (B and C) High-frequency echocardiography was performed to evaluate cardiac function. (D) Kaplan–Meier survival curves showing the survival of DOX-stressed adult fish after drug administration in the early phase. n=15~25. (E) Schematics of the experimental procedure for drug administration in the late phase of aAIC. (F and G) High-frequency echocardiography was performed 8 wpi to evaluate cardiac functions. (H) Kaplan–Meier survival curves showing the survival of DOX-stressed adult zebrafish after

drug administration in the late phase. n=15~25. Log-rank test was used in (D) and (H) for comparisons; one-way ANOVA followed by post hoc Tukey's test in (B), (C), (F) and (G). wpi, weeks after DOX injection. WT, wild type; DOX, doxorubicin.

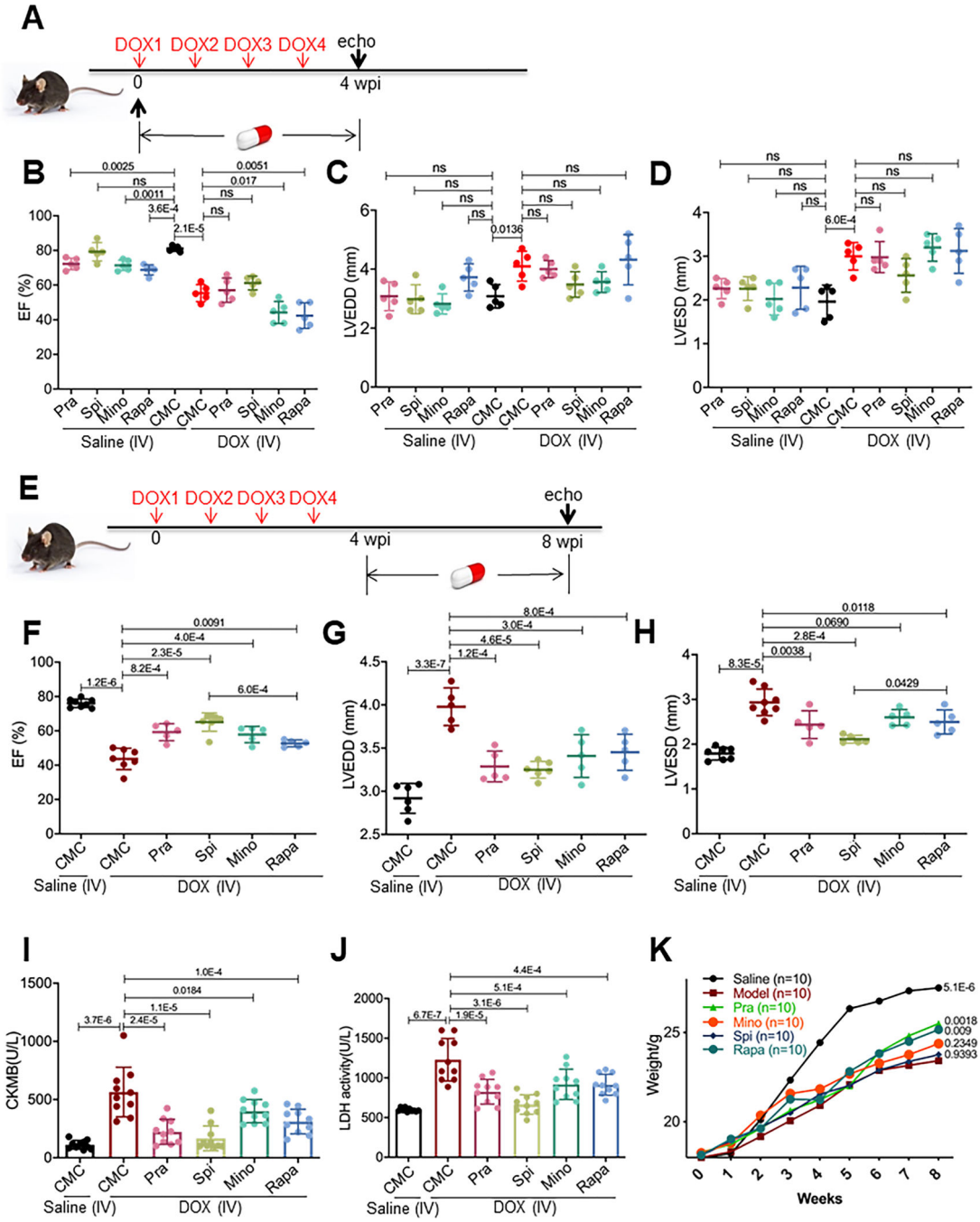

Fig 6. Top-ranking FAAs, including spironolactone (Spi), pravastatin (Pra), minoxidil (Mino) and rapamycin (Rapa), exerted therapeutic effects in a mouse AIC model in a time-dependent fashion.

(A) Schematics of the experimental procedure for drug administration in the early phase of the mouse AIC model. (B to D) Echocardiography was performed to evaluate cardiac functions. (n=5) (E) Schematics of the experimental procedure for drug administration to the AIC model mice in the late phase. (F to H) Echocardiography was performed to evaluate cardiac functions. (n=5) (I and J) All four drugs attenuated the increase in serum LDH and CKMB. (n=8). (K) All four drugs reversed body weight loss in the AIC model mice. (n=10).

One-way ANOVA followed by post hoc Tukey's test was used. Log-rank test was used in (K) for comparisons with the model group. We applied a 0.5% aqueous solution of sodium carboxymethylcellulose (CMC) as a vehicle.

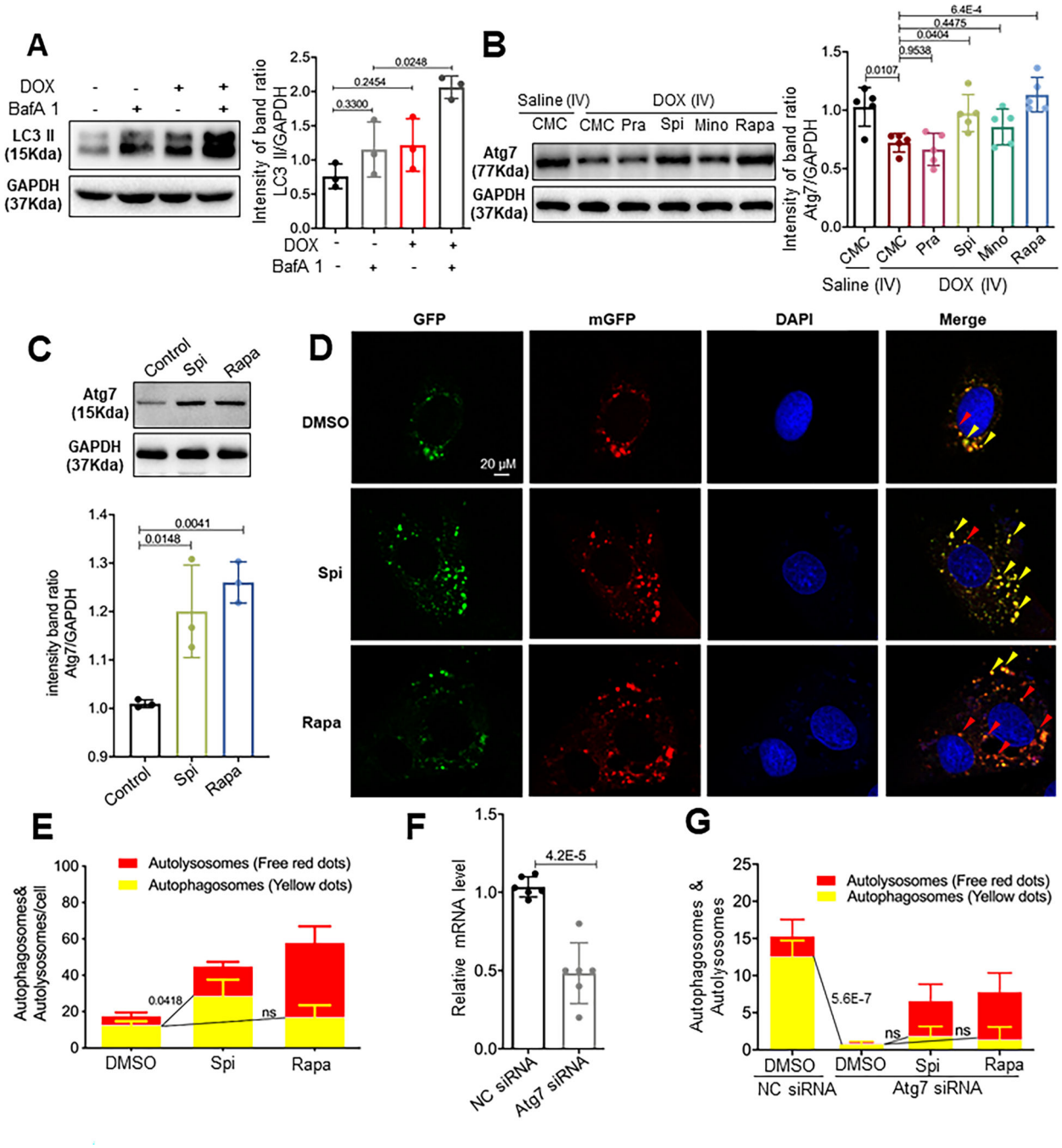

Fig 7. Spironolactone (Spi) and rapamycin (Rapa) activated autophagosome formation in an Atg7-dependent fashion.

(A) Representative Western blot and quantification of the relative amounts of LC3-II in the hearts from mice injected with a single bolus of DOX. Activated LC3-II and an increased response to BafA1 (n=5/treatment) were observed. (B) Representative Western blots and quantification of Atg7 from the hearts of mice administered the four drugs daily in the later phase. (C) Representative Western blot and quantification of Atg7 from the H9C2 cardiac cell line. Spi and Rapa induced an increase in Atg7 protein levels. (D) H9C2 cells were transiently transfected with mRFP-GFP-LC3 adenovirus and then treated with

Spi and Rapa. Representative images of GFP-LC3 and mRFP-LC3 puncta are shown. (E) Quantification of the yellow puncta (autophagosomes) and red puncta (autolysosomes) is shown in (D). (F) qRT-PCR was used to confirm that Atg7 transcripts were reduced by Atg7 siRNA. (G) Quantitative analysis of the yellow puncta (autophagosomes) and red puncta (autolysosomes) showing that Atg7 siRNA ablates the induction of autophagosomes induced by Spi or Rapa. Kruskal-Wallis test was used followed by post hoc Tukey's test in (A) and (C); one-way ANOVA followed by post hoc Tukey's test in (B), (E) and (G); student's test in (F).

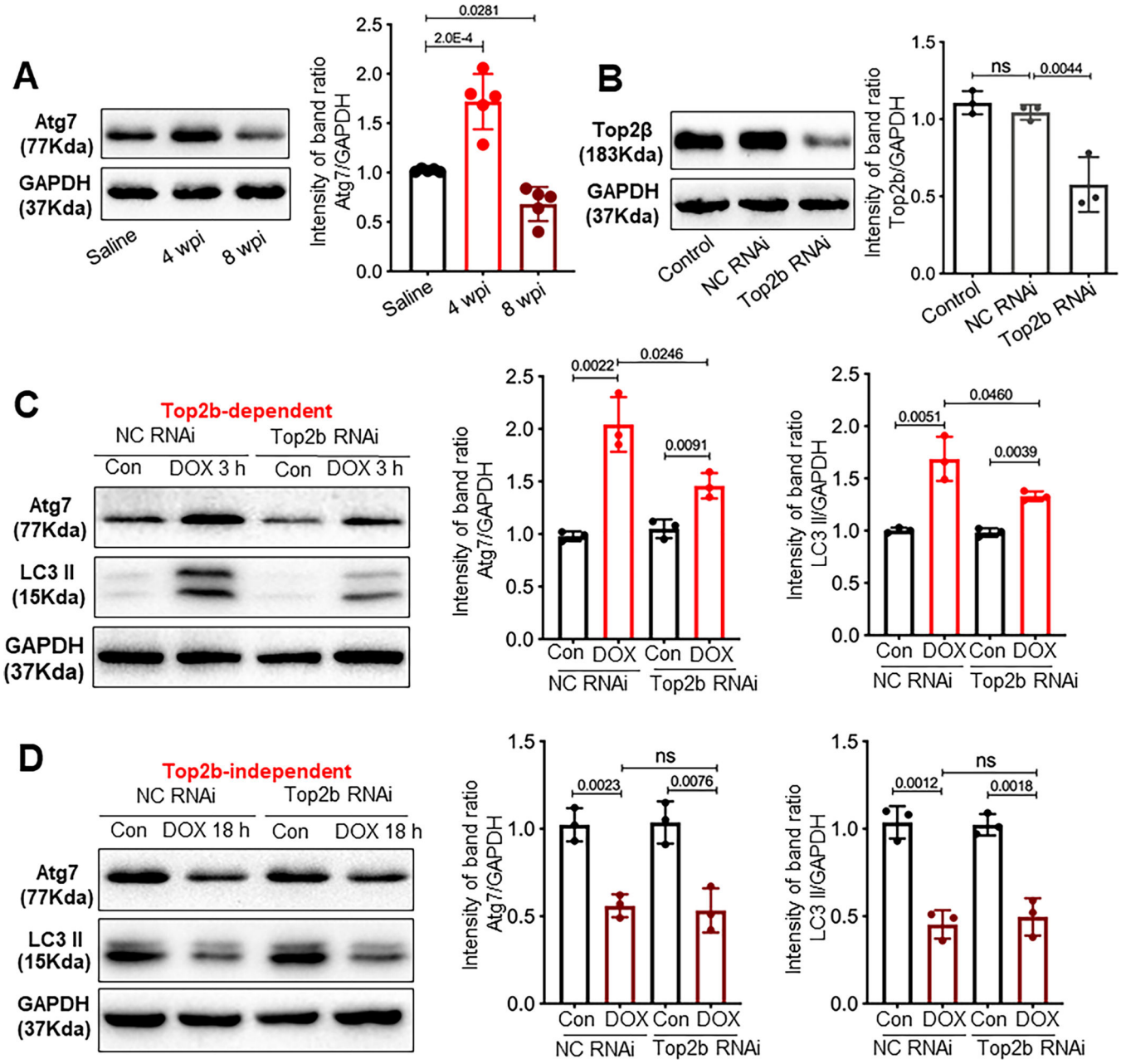

Fig 8. Top2b is required for atg7-mediated autophagy in the early but not the late phase of AIC.

(A) Temporal changes of Atg7 protein level post the first dose of DOX in the mouse AIC model. N=5 mice per group. 4 wpi would be considered as the early phase, because it is equal to 1 week post the last dose of DOX. (B) H9C2 cells were transfected with the indicated siRNA. Cell lysates were analyzed by Western blots to check the knock down effects. H9C2 cells transfected with NC RNAi or Top2b RNAi were treated by DOX for 3 h (C) or 18 h (D), then levels of Atg7 and LC3II were examined by Western blots. Kruskal-Wallis test was used followed by post hoc Tukey's test.